

Tunable Acoustic Lenses based on Phononic Crystals

Fatemeh Ahmadzadeh^{a*}, Ali Bahrami^a

^a*Optoelectronic and Nanophotonic Research Lab. (ONRL), Faculty of Electrical Engineering, Sahand university of Technology, Tabriz, Iran.*

* Corresponding author e-mail: fa_ahmadzadeh98@sut.ac.ir

Abstract

A two-dimensional gradient-index phononic crystal (GRIN PnC) of steel cylinders in an ethanol matrix was designed and simulated for $\lambda \geq 6a$ at room temperature. The hyperbolic secant profile of the refractive index is obtained by changing the scatterers radius of the structure in the transverse direction to gradually refract the waves. The finite element method is used to calculate the effective refractive index in each row of the structure and to investigate the propagation of acoustic waves in the gradual medium. With the help of gradient structure equations, the analytical beam trajectories were obtained and compared with the wave propagation results. The effect of temperature on the first band and thermal adjustment of the focal point for 0°C and 50°C have been investigated. The obtained results show that it is possible to shift the focal point at a certain frequency due to the changes of the effective refractive indices of the cylinders in the transverse positions for the calibration applications.

Keywords: Phononic crystal lens; Hyperbolic secant profile; Thermal tuning; Focal point shift.

1. Introduction

Phononic crystals are the periodic structures of scatterers in a matrix for controlling and manipulating mechanical waves, first introduced in 1993 [1, 2]. The main focus at first was due to the band gap at $\lambda \approx a$; in this frequency range, waves were not allowed to pass into the structure and the structure acts like a great mirror. Controlling the propagation of waves in linear media is important because it allows the design of waveguide [3], beam splitters [4], switches [5], multiplexers [6], sensor applications [7], frequency filters [8], cloaking devices [9, 10], acoustic and elastic lenses [11-16], and applications of phononic crystals in acoustofluidics [17-19]. The topological transport of elastic wave in phononic crystal provides potential in information processing, reinforcing nondestructive testing (NDT), and high sensitivity sensing [20-23]. Cervera et al. had presented a phononic crystal of an aluminum cylinder in air, which allowed sound waves to be refracted [11]. They also found the relationship between sound velocity and filling ratio; as the filling ratio increases, the speed of sound in the crystal decreases. Hakanson introduced a flat acoustic lens with the same material, in which

the cylinders were genetically positioned so that maximum sound could be obtained at the focal point [12].

It has been shown that flat phononic crystals lenses show negative refraction in partial phononic band gaps, where PnCs have high anisotropy that can be used to design acoustic lenses but have a limited operating range [24, 25]. Gradient-index (GRIN) structures were studied first for acoustic waves [25] and then for elastic waves [26]. These structures can be implemented by geometric changes such as gradual changes in the filling ratio of scatterers [13, 14, 27], the variation in the lattice constant while keeping the size of scatterers [28, 29], angular changes in the scatterers [30, 31], the thickness of the slabs [32], and also by gradual changes in material properties [26, 33]. The structure that Torrent presented for acoustic waves consisted of 9-layer slab of gel and rigid cylinders in air [25] and the choice of materials was such that the highest impedance matching was achieved between the scatterers and the matrix material. Lin et al. then proposed a gradual structure for elastic waves that used gradual material changes [26]; the frequency range obtained in this work was greater than structures with negative refraction. Lenses with a positive refractive index work in the first pass band and have been noted for their easy fabrication of flat phononic crystal. However, phononic crystal lenses were introduced for the designable focal length in the second pass band where the equal frequency contours (EFCs) move inwards, which indicates a negative group velocity [34].

Many studies have been presented on different methods for tuning the band gap of phononic crystals, and apply heat to the structure is one of these methods. Here, by changing the radius of the scatterers, a two-dimensional gradient-index phononic crystal is designed so that the effects of temperature can shift the focal point. In section 2, the theoretical background will be presented. Its design principles are presented in section 3 and with the help of the finite element method, the band diagram of unit cell and also the wave propagation inside the structure are shown. Finally, the effects of temperature on the structure as well as the focal length are discussed.

2. Theoretical Background

There are two approaches to PnC lens design: positive and negative refract. In this paper, positive refract and gradient-index profiles are used. Parabolic profiles are used in optical lenses, but in hyperbolic secant profile, due to non-approximation, the focal point has less aberration [26]. For this two-dimensional structure, the refractive index profile in transverse direction is defined as [26]:

$$n(y) = n_{\max} \operatorname{sech}(\theta y) \quad (1)$$

where n_{\max} is the refractive index in the middle of the lens, which is the maximum refractive index and θ is the gradient coefficient:

$$\theta = \frac{1}{h} \cosh^{-1}\left(\frac{n_{\max}}{n_{\min}}\right) \quad (2)$$

here h is half the height of the lens and n_{\min} is the refractive index at the edge of the lens. According to Snell's law, the waves were bent to the maximum refractive index to converge at a focal point. The waves begin to propagate in parallel on the other side. The path of the propagating waves inside this GRIN structure can be solved as follows [36]:

$$y(x) = \frac{1}{\theta} \sinh^{-1}[u_0 H_f(x) + \dot{u}_0 H_a(x)] \quad (3)$$

where u_0 is the hyperbolic space at $x = 0$, \dot{u}_0 is the derivative of u_0 with respect to x , and $H_f(x)$ and $H_a(x)$ are the positions of axial and field rays. The trajectory of the waves inside the GRIN structure is determined according to Eq. (3) and the focal length can be calculated [26]:

$$focal \ length = \frac{\pi}{2\theta}. \quad (4)$$

A 2D GRIN phononic crystal is an example of a discrete structure in transverse direction that each row can be considered as a homogeneous and isotropic media [26]. This discrete structure is realized by gradually changing the radii of the scatterers; then the effective refractive index is calculated for each scatterers's radius and according to Eq. (1) a refractive index profile can be designed. The effective refractive index at a specified frequency is calculated as follows [26]:

$$n_{eff} = \frac{n_{\Gamma X} + n_{\Gamma M}}{2} \quad (5)$$

where $n_{\Gamma X}$ and $n_{\Gamma M}$ are refractive indices along the ΓX and ΓM directions (high symmetry points of PnC band structure), respectively [26]:

$$n_{\Gamma X} = \frac{C}{v_{\Gamma X}} = \frac{C}{\partial\omega/\partial k_{\Gamma X}}, \quad n_{\Gamma M} = \frac{C}{v_{\Gamma M}} = \frac{C}{\partial\omega/\partial k_{\Gamma M}} \quad (6)$$

where v is the group velocity in different directions and C is the sound velocity in a matrix material.

In the next section, First, the large and small radii of the cylinders as well as half the height of the lens (i. e. h) are determined in order to obtain a profile for the refractive index according to the Eq. (1), then the closest refractive indices (corresponding radius) will be calculated with the help of Eq. (5) and Eq. (6).

3. Design Procedure

Each unit cell contains steel rods in ethanol and material parameters at room temperature are given in Table 1. By defining the reduced frequency as $\Omega = fa/C$ (where f is the frequency, a is the lattice constant of the PnC and C is the sound velocity in matrix material) the structure was designed for $\Omega = 0.17$, which corresponds to wavelength $\lambda = 6a$.

Table 1. Material properties of the proposed phononic crystal lens at 25°C.

Steel	$\rho(g/cm^3)$	$E(GPa)$	ν
	7.870	215	0.3
Ethanol	$\rho(g/cm^3)$	$C(km/s)$	
	0.785	1.14	

The first pass band for the selected radii is shown in Fig. 1. It is important to note that the presented lens has a positive refract ($\Omega = 0.17$).

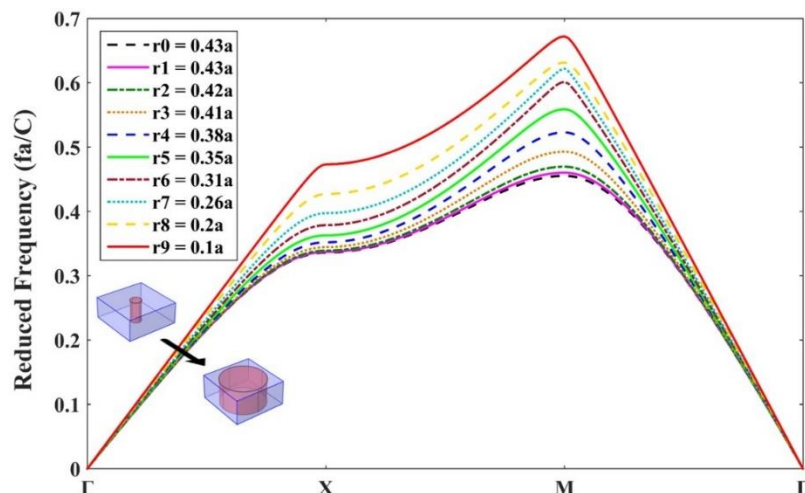


Figure 1. The band diagram for different rows that have different radii of the GRIN PnC

As can be seen, the radii increases (from $r = 0.1a$ to $r = 0.42a$), first band comes to lower frequencies, which increases the refractive index (decreases the group velocity) at reduced frequency of $\Omega = 0.17$. The refraction of the wave can be conveniently visualized with the EFC; for an isotropic medium the EFCs are perfect circles since the magnitude of the wave vector is independent of the direction of propagation [39].

4. Simulation Results

The final structure consists of 60 layers in the x direction and 19 rows in the y direction and the lattice constant was set as 7 mm is shown in Fig. 2, as can be seen, the radius towards the edge of the lens is decreasing. To analyse the ability of the lens to manipulate waves and focus them, the propagation of waves in a two-dimensional space was obtained using the FE numerical method (COMSOL Multiphysics). The entire domain was surrounded by absorbent at the boundaries to avoid reflections in the simulation domain and a line source was placed at left side of the structure.

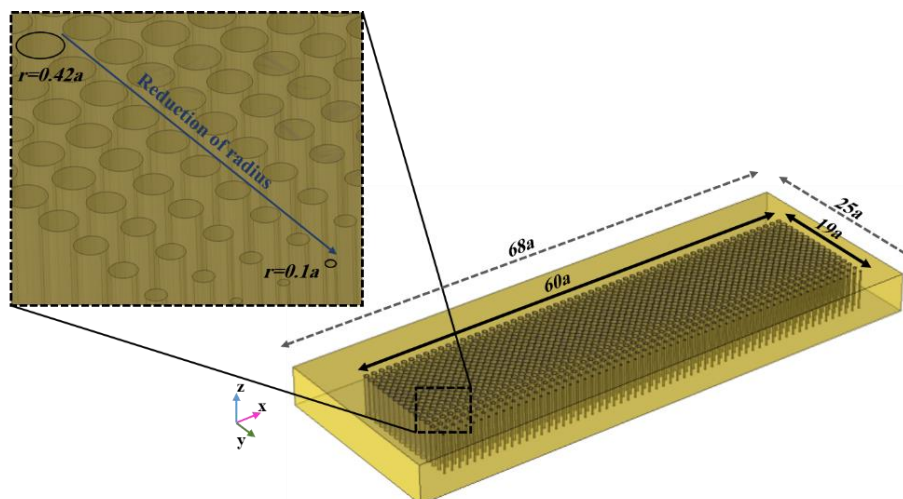


Figure 2. 3D schematic view of a GRIN phononic crystal lens

According to Eq. (4), with increasing gradient coefficient, the focal point shifts to lower places, it is also found that the gradient coefficient and frequency are directly related, so with increasing frequency, θ increases (see Fig. 3(a)).

Figure 3(b) and (c) shows the numerical simulation for propagation of acoustic waves that pressure is normalized to its maximum value. At $\Omega = 0.17$, the beam trajectory calculated from Eq. (3) and it is shown in Fig. 3(b).

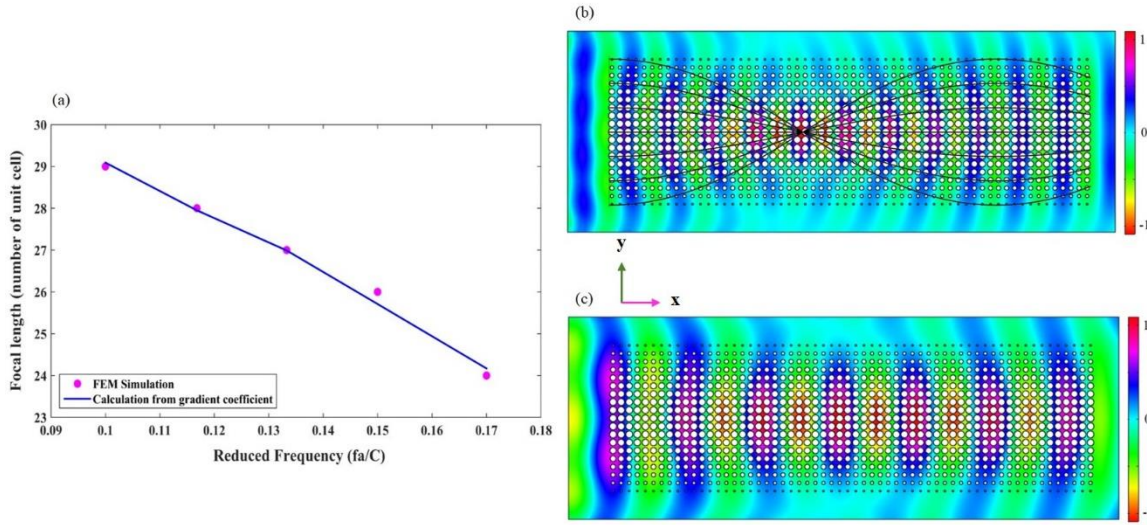


Figure 3. (a) The focal length of GRIN PnC lens versus the reduced frequency. Numerical simulation of FE for propagation of acoustic waves in gradient-index structures at a reduced frequency of (b) $\Omega = 0.17$ and (c) $\Omega = 0.1$. The black line in (b) show the beam trajectory

According to Fig. 3(b), the plane waves of a linear source located in $-5a$ are gradually refracted to focus at $24a$, this corresponds to the value of theory $\pi/2\theta = 24.15$ with $\theta = 0.0650$. The acoustic pressure field at the focus spot is more than 2.9 times higher than the incident wave. Figure 3(c) shows the propagation of waves at frequency $\Omega = 0.1$ that the waves gradually bend toward the center and focus in $29a$, which corresponds to the value of the theory.

5. Thermal Tuning

By examining the effect of temperature on the structure, the possibility of shifting the focal point for temperatures of 0°C and 50°C by applying heat to the matrix material is investigated. Note that at the investigated temperatures the effect on steel is small and can be ignored. In Ref. [40], the dependence of sound speed and mass density of ethanol on temperature has been investigated.

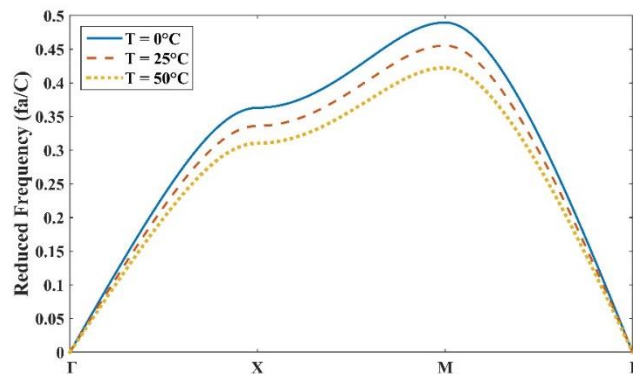


Figure 4. The band diagram at different temperatures for $r = 0.42a$

Figure 4, plotted for $r = 0.42a$ at three different temperatures, shows that as the temperature increases, the first band shifts to lower frequencies; in other words, by increasing or decreasing the temperature at a certain frequency, a different refractive index can be obtained. As a result, the

hyperbolic secant profile of the refractive index will have different gradient coefficient at different temperatures. Figure 5(a) shows the simulation results at 0°C for the design frequency, where the focal point corresponds to the theoretical value.

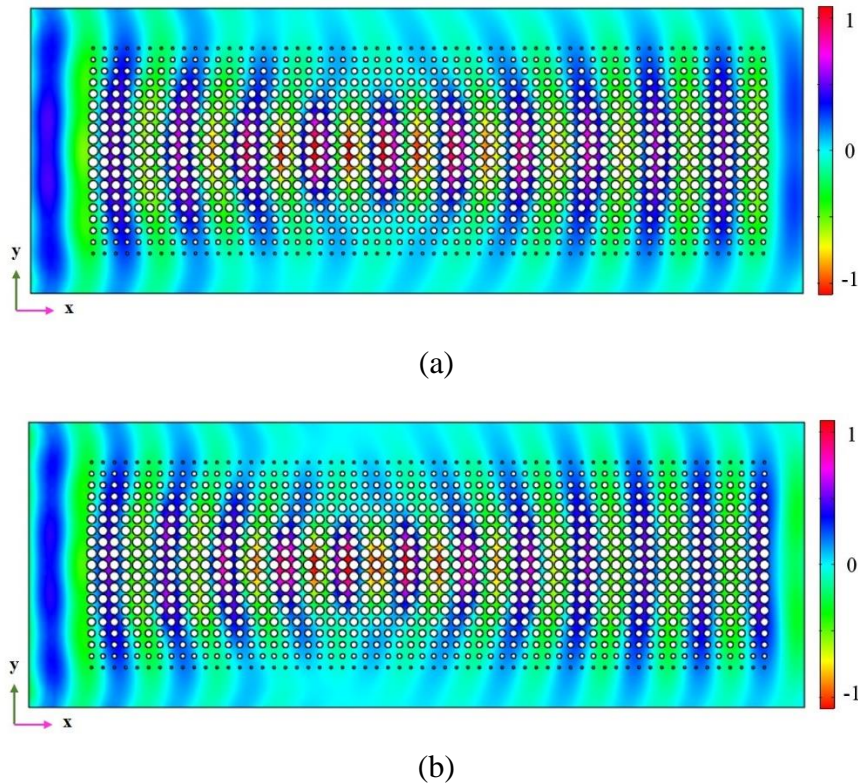


Figure 5. Numerical simulation for propagation of acoustic waves in gradient-index structures at a reduced frequency of $\Omega = 0.17$ for (a) $T = 0^\circ\text{C}$ and (b) $T = 50^\circ\text{C}$

It was observed that as the temperature decreased, the focus point shifted upwards. To increase the temperature by as much as 25°C, find that the focal point shifts downwards as shown in Fig. 5(b).

6. Conclusions

In this paper, a two-dimensional phononic crystal lens with a gradient index was designed and simulated to refract sound waves and converge them at a focal point. Due to high anisotropy at high frequencies, the structure was designed for $\lambda \geq 6a$. The refractive index profile obtained from the hyperbolic secant relation causes minimal aberration in focal length. Then, with the help of the effects of temperature on the first band, the possibility of shifting the focal point was investigated. The finite element method has been used to numerically simulate the structure.

REFERENCES

1. M. S. Kushwaha, P. Halevi, L. Dobrzynski, B. Djafari-Rouhani, “Acoustic band structure of periodic elastic composites”, *Physical Review Letters* **71**, 2022 (1993).
2. M. Sigalas, EN. Economou, “Band structure of elastic waves in two dimensional systems”, *Solid State Commun* **86**, 141 (1993).

3. A. Khelif, B. Djafari-Rouhani, J. O. Vasseur, P. A. Deymier, "Transmission and dispersion relations of perfect and defect-containing waveguide structures in phononic band gap materials", *Physical Review B* **68**, 024302 (2003).
4. Y. Tang, Y. Zhu, B. Liang, J. Yang, J. Yang, J. Cheng, "One-way Acoustic Beam Splitter", *Scientific reports* **8**, 1-6 (2018).
5. A. Bahrami, M. Alinejad-Naini, F. Motaei, "A proposal for 1×4 phononic switch / demultiplexer using composite lattices", *Solid State Communications* **326** (2021).
6. B. Rostami-Dogolsara, M. Moravvej-Farshi, F. Nazari, "Designing switchable phononic crystal-based acoustic demultiplexer", *IEEE transactions on ultrasonics, ferroelectrics, and frequency control* **63**, 1468-1473 (2016).
7. H. Gharibi, A. Khaligh, A. Bahrami, H.B Ghavifekr, "A very high sensitive interferometric phononic crystal liquid sensor", *Journal of Molecular Liquids* **296**, 111878 (2019).
8. Y. Pennec, J. Vasseur, B. Djafari-Rouhani, L. Dobrzynski, P.A. Deymier. "Two-dimensional phononic crystals: Examples and applications", *Surface Science Reports* **65**, 229-291 (2010).
9. S. A. Cummer, D. Schurig, "One path to acoustic cloaking", *New Journal of Physics* **9**, p. 45 (2007).
10. D. Torrent, J. Sanchez-Dehesa, "Acoustic cloaking in two dimensions: a feasible approach", *New Journal of Physics* **10**, 063015 (2008).
11. F. Cervera, L. Sanchis, J. V. Sanchez-Perez, R. Martinez-Sala, C. Rubio, F. Meseguer, "Refractive Acoustic Devices for Airborne Sound", *Physical review letters* **88**, 023902 (2001).
12. A. Hakansson, F. Cervera, J. Sanchez-Dehesa, "Sound focusing by flat acoustic lenses without negative refraction", *Applied Physics Letters* **86**, 054102 (2005).
13. A. Climente, D. Torrent, J. Sanchez-Dehesa, "Sound focusing by gradient index sonic lenses", *Applied Physics Letters* **97**, 104103 (2010).
14. T. P. Martin, M. Nicholas, G. J. Orris, L.W. Cai, D. Torrent, J. Sanchez-Dehesa, "Sonic gradient index lens for aqueous applications", *Applied Physics Letters* **97**, 113503 (2010).
15. A. Sukhovich, L. Jing, J. H. Page, "Negative refraction and focusing of ultrasound in two-dimensional phononic crystals", *Physical Review B* **77**, 014301 (2008).
16. K. Deng, Y. Ding, Zh. He, Zh. Liu, H. Zhao, J. Shi, "Graded negative index lens with designable focal length by phononic crystal", *Applied Physics* **42**, 185505 (2009).
17. R. Wilson, J. Reboud, Y. Bourquin, S. L. Neale, Y. Zhang, J. M. Cooper, "Phononic crystal structures for acoustically driven microfluidic manipulations", *Lab on a Chip* **11**, 323-328 (2011).
18. J. C. Hsu, Y. D. Lin, "Microparticle concentration and separation inside a droplet using phononic crystal scattered standing surface acoustic waves", *Sensors and Actuators A: Physical* **300**, 111651 (2019).
19. F. Li, F. Cai, L. Zhang, Z. Liu, F. Li, L. Meng, J. Wu, J. Li, X. Zhang, H. Zheng, "Phononic crystal enabled dynamic manipulation of microparticles and cells in an acoustofluidic channel", *Physical Review Applied* **13**, 044077 (2020).
20. S. Y. Huo, J. J. Chen, H. B. Huang, Y. J. Wei, Z. H. Tan, L. Y. Feng, X. P. Xie, "Experimental demonstration of valley-protected backscattering suppression and interlayer topological transport for elastic wave in three-dimensional phononic crystals", *Mechanical Systems and Signal Processing* **154**, 107543 (2021).
21. S. Y. Huo, J. J. Chen, H. B. Huang, G. L. Huang, "Simultaneous multi-band valley-protected topological edge states of shear vertical wave in two-dimensional phononic crystals with veins", *Scientific reports* **7**, 1-8 (2017).
22. S. Y. Huo, J. J. Chen, L. Y. Feng, H. B. Huang, "Pseudospins and topological edge states for fundamental antisymmetric Lamb modes in snowflakelike phononic crystal slabs", *The Journal of the Acoustical Society of America* **146**, 729-735 (2019).
23. S. Yang, J. H. Page, Z. Liu, M. L. Cowan, C. T. Chan, P. Sheng, "Focusing of sound in a 3D phononic crystal", *Physical Review Letters* **93**, 024301 (2004).
24. L. Feng, X. P. Liu, Y. B. Chen, Z. P. Huang, Y. W. Mao, Y.F. Chen, J. Zi, Y. Y. Zhu, "Negative refraction of acoustic waves in two-dimensional sonic crystals", *Physical Review B* **72**, 033108 (2005).
25. D. Torrent, J. Sanchez-Dehesa, "Acoustic metamaterials for new two-dimensional sonic devices", *New Journal of Physics* **9**, 323 (2007).

26. S. C. S. Lin, T. J. Huang, J. H. Sun, T. T. Wu, "Gradient-index phononic crystals", *Physical Review B* **79**, 094302 (2009).
27. M. J. Chiou, Y. C. Lin, T. Ono, M. Esashi, S. L. Yeh, T. T. Wua, "Focusing and waveguiding of Lamb waves in micro-fabricated piezoelectric phononic plates", *Ultrasonics* **54**, 1984-1990 (2014).
28. T. P. Martin, C. J. Naify, E. A. Skerritt, C. N. Layman, M. Nicholas, D. C. Calvo, G. J. Orris, "Transparent gradient index lens for underwater sound based on phase advance", *Physical Review Applied* **4**, 034003 (2015).
29. S. C. S. Lin, B. R. Tittmann, T. J. Huang, "Design of acoustic beam aperture modifier using gradient-index phononic crystals", *Journal of applied physics* **111**, 123510 (2012).
30. Y. Tian, Z. Tan, X. Han, W. Li, "Phononic crystal lens with an asymmetric scatterer", *Journal of Physics D: Applied Physics* **52**, 025102 (2018).
31. Z. Tan, Y. Wei, Y. Tian, X. Han, "Gradient negative refraction index phononic crystal lens with a rotating scatterer", *Materials Research Express* **6**, 096203 (2019).
32. A. Climente, D. Torrent, J. Sanchez-Dehesa, "Gradient index lenses for flexural waves based on thickness variations", *Applied Physics Letters* **105**, 064101 (2014).
33. S. C. S. Lin, B. R. Tittmann, J. H. Sun, T. T. Wu, T. J. Huang, "Acoustic beamwidth compressor using gradient-index phononic crystals", *Journal of Physics D: Applied Physics* **42**, 185502 (2009).
34. K. Deng, Y. Ding, Z. He, Zh. Liu, H. Zhao, J. Shi, "Graded negative index lens with designable focal length by phononic crystal", *Journal of Physics D: Applied Physics* **42**, 185505 (2009).
35. A. Khelif, A. Adibi, *Phononic Crystals*, Springer, New York, (2016).
36. C. Gomez-Reino, M. V. Perez, C. Bao, *Gradient-index Optics: Fundamentals and Applications*, 5th ed, Springer, Berlin, (2002).
37. E. Centeno, D. Cassagne, J. P. Albert, "Mirage and superbending effect in two-dimensional graded photonic crystals", *Physical Review B* **73**, 235119 (2006).
38. M. Ke, Z. Liu, C. Qiu, W. Wang, J. Shi, W. Wen, P. Sheng, "Negative-refraction imaging with two-dimensional phononic crystals", *Physical Review B* **72**, 064306 (2005).
39. P. A. Deymier, *Acoustic Metamaterials and Phononic Crystals*, 1th ed, Springer, Berlin, (2013).
40. W. Wilson, D. Bradley, "Speed of sound in four primary alcohols as a function of temperature and pressure", *The Journal of the Acoustical Society of America* **36**, 333-337 (1964).